

Vehicle-group-based Crash Risk Formation and Propagation Analysis for Expressways

Tianheng Zhu, Ling Wang, Yiheng Feng, *Member, IEEE*, Wanjing Ma and Mohamed Abdel-Aty, *Senior Member, IEEE*

Abstract—Previous studies in predicting crash risk primarily associated the number or likelihood of crashes on a road segment with traffic parameters or geometric characteristics of the segment, usually neglecting the impact of vehicles' continuous movement and interactions with nearby vehicles. Advancements in communication technologies have empowered driving information collected from surrounding vehicles, enabling the study of group-based crash risks. Based on high-resolution vehicle trajectory data, this research focused on vehicle groups as the subject of analysis and explored risk formation and propagation mechanisms considering features of vehicle groups and road segments. Several key factors contributing to crash risks were identified, including past high-risk vehicle-group states, complex vehicle behaviors, high percentage of large vehicles, frequent lane changes within a vehicle group, and specific road geometries. A multinomial logistic regression model was developed to analyze the spatial risk propagation patterns, which were classified based on the trend of high-risk occurrences within vehicle groups. The results indicated that extended periods of high-risk states, increase in vehicle-group size, and frequent lane changes are associated with adverse risk propagation patterns. Conversely, smoother traffic flow and high initial crash risk values are linked to risk dissipation. Furthermore, the study conducted sensitivity analysis on different types of classifiers, prediction time intervals and adaptive TTC thresholds. The highest AUC value for vehicle-group risk prediction surpassed 0.93. The findings provide valuable insights to researchers and practitioners in understanding and prediction of vehicle-group safety, ultimately improving active traffic safety management and operations of Connected and Autonomous Vehicles.

Index Terms—Crash risk formation, Crash risk propagation, Vehicle-group-based safety analysis, Vehicle trajectory data

This study is supported by National Natural Science Foundation of China (No. 52102415, 52372333, 52325210) and Fundamental Research Funds for the Central Universities (2023-4-YB-05). (Corresponding author: Ling Wang.)

Tianheng Zhu was with the College of Transportation Engineering, Tongji University, Shanghai, 201804 China. He is now with the Lyles school of Civil Engineering, Purdue University, Indiana, 47907 USA (e-mail: zhu1230@purdue.edu).

Ling Wang is with the College of Transportation Engineering, Tongji University, Shanghai, 201804 China (e-mail: wang_ling@tongji.edu.cn).

Yiheng Feng is with the Lyles School of Civil Engineering, Purdue University, Indiana, 47907 USA (e-mail: feng333@purdue.edu).

Wanjing Ma is with the College of Transportation Engineering, Tongji University, Shanghai, 201804 China (e-mail: mawanjing@tongji.edu.cn).

Mohamed Abdel-Aty is with the Department of Civil, Environmental and Construction Engineering, University of Central Florida, Florida, 32816 USA (e-mail: M.Aty@ucf.edu).

Color versions of one or more of the figures in this article are available online at <http://ieeexplore.ieee.org>

I. INTRODUCTION

The evolution of communication, sensing and computing technologies have significantly transformed vehicle crash-avoidance strategies. Unlike traditional Active Traffic Management (ATM) techniques such as Variable Speed Limit (VSL) and Ramp metering (RM), Connected and Autonomous Vehicles (CAVs) offer superior road safety enhancements, including traffic jam and incident reporting, collision warning, and collision avoidance, facilitated by vehicle-to-everything (V2X) communication [1]. Notably, Ma et al. [2] developed a suite of CAV-oriented ATM approaches, encompassing VSL, RM, and coordinated VSL-RM system, which demonstrated a 2.84-15.92% enhancement in expressway safety benefits. The timely deployment of CAV-based ATM strategies in high-risk scenarios is essential, underscoring the importance of accurately determining real-time crash risks.

Previous studies in predicting crash risk focused on road segments as their subject of analysis [3-6], potentially overlooking the impact of vehicles' continuous movement and interactions with surrounding vehicles. With the advancement of V2X technology, the presence of other vehicles in the immediate neighborhood can be observed [7], facilitating the study of group-based crash risks. This study utilized high-resolution trajectory data, representative of connected-vehicle data, and leveraged vehicle group trajectories and microscopic variables collected from vehicle groups to capture the interactions between vehicles and the cascading effect of current vehicle states on future crash risks.

Most previous research has concentrated on risk prediction, with a notable gap in the examination of crash risk propagation. This study classified crash risk propagation patterns based on the trend of high-risk occurrences within vehicle groups and further explored the factors associated with different propagation patterns.

This paper is organized into seven sections. The second section presents the literature review. The third section details the methodologies for constructing vehicle-group trajectories, statistical models, quantification of vehicle-group risk, and defining risk propagation patterns. The fourth section presents the data preparation. The fifth section presents results on risk formation and propagation analysis, sensitivity analysis regarding different classifiers, prediction time intervals, and adaptive Time-to-Collision (TTC) thresholds, and finally, the sixth section summarizes the findings, conclusions,

applications, and limitations of the study.

II. LITERATURE REVIEW

There have been plenty of studies on crash risks for expressways or highways. Most of them focused on road segments as their subject of analysis, with potential crash precursors extracted from the current, upstream, and downstream segments [3-6]. However, due to vehicles' continuous movement, the vehicle state at one point can influence future risks. Meanwhile, crash risks often result from interactions between vehicles over time. These spatiotemporal characteristics of crash risks are critical in vehicle trajectory control [8, 9], crash likelihood assessment [10], driving intention analysis [11], and traffic flow analysis [12], highlighting their importance in understanding crash risk. Wang et al. [13] attempted to address this by deriving historical vehicle positions through space-mean-speed and constructing a quasi-vehicle trajectory. Traffic data collected from the road segments of these positions were utilized to understand crash risks. However, the input data collected from fixed traffic sensors were still at the aggregated level, e.g., volume difference. The aggregated data lacked detail on individual vehicles and the interactions between them, limiting its effectiveness for in-depth risk analysis. Arbabzadeh et al. [14] incorporated traffic flow information surrounding target vehicles in their crash risk prediction model, yet this method still did not fully capture vehicle interactions. With the advancement of V2X technology, the presence of other vehicles in the immediate neighborhood can be observed [7], which enables detailed vehicle data collection. The high-resolution data allows for the study of vehicle groups as the subject of analysis. In prior studies, vehicles were grouped based on their locations [15] or potential crash risks between vehicles [16, 17], aiding in the identification of chain-conflicts [16] and quantification of crash risks [15]. Nevertheless, these studies often focused on individual timestamps, paying minimal attention to the dynamics of vehicle groups. Therefore, further investigation into moving vehicle groups and the underlying risk mechanisms is warranted.

The input data of previous studies was also limited. Fixed-location traffic data was widely used. It was usually collected based on a 30-minute time window prior to a crash occurrence and aggregated into a time interval of 5 minutes [4, 18-21] or 6 minutes [22]. Recent trends favor defining a 5 to 10-minute window preceding a crash as the crucial pre-crash period [23, 24]. However, aggregated traffic data cannot provide high-resolution information, prompting the use of simulation data to recreate specific traffic conditions [25] and generate trajectory data [26]. Despite this, simulations may not capture the full complexity and variability of reality, leading to potential biases in results. To address these limitations, high-fidelity trajectory datasets like NGSIM, HighD and CitySim, were used in studies [27-29]. However, datasets like NGSIM and HighD are constrained by their limited scope in road section types, traffic states, and volumes, etc., making them difficult to represent a diverse range of traffic scenarios and road

conditions.

Crash risk precursors are multifaceted, influenced by a variety of factors. Commonly utilized traffic flow variables in crash risk prediction include statistics or logarithmic transformations of speed, flow and occupancy, as well as their differences in space or various time slices [23]. Additionally, crash risk correlates with roadway geometric characteristics [3], weather [30, 31], and driving behaviors [32]. However, the reliance on aggregated traffic data has led to a lack of detail in selecting and analyzing these crash precursors.

Previous research predominantly concentrated on predicting crash occurrences [33-35]. However, there has been a notable gap in examining the propagation of crash risks. Analyzing how crash risks propagate and identifying contributing factors are crucial for comprehending risk mechanisms and effectively mitigating their impact.

In summary, none or little literature analyzed crash risks based on vehicle-group trajectories with high-resolution data. Furthermore, the selection of crash precursors was largely macroscopic and the analysis of risk propagation was not considered. To address these gaps, this study leveraged vehicle group trajectories to capture the spatiotemporal characteristics of crash risks. Microscopic variables were collected from individual vehicles within the MAGIC dataset [36]. With the proposed methods and data, this study provides a unique and deep insight into the formation and propagation of crash risks. The findings could benefit the estimation and prediction of crash risks of moving vehicle groups and provide guidance for the group-level crash-avoidance control strategies of CAVs.

III. METHODS

A. Vehicle-group Segmentation and Matching Method

In this study, vehicle groups were selected as the primary subjects to effectively capture the spatiotemporal characteristics of crash risks. The initial step involved segmenting vehicle groups at individual timestamps, using the Time-to-Collision (TTC) metric as a key criterion. This was followed by pairing vehicle groups from successive timestamps that exhibited similar features, thereby creating continuous vehicle-group trajectories.

1) Surrogate Safety Measure

Surrogate safety measure (SSM) is an alternative method of assessing safety that relies on the analysis of safety-critical events known as traffic conflicts [37]. In this study, Time-to-Collision (TTC) [38] was adopted as a SSM to quantify crash risks. It is defined as the remaining time for a collision to occur, under the assumption that both the leading and following vehicles continue at their current speeds and trajectories. The formula of TTC is shown in **Eq. (1)**. TTC is readily measurable [39], relying solely on vehicles' position and speed data. In contrast, more advanced SSMs like Modified Time-to-Collision (MTTC) [40] necessitate details such as acceleration, which can be challenging to accurately gather, particularly from drone-collected datasets as used in our study. Additionally, considering TTC's wide recognition

as a prevalent SSM [11], its implementation in our research underlines the study's practical relevance and applicability. Nonetheless, TTC might have limitations in precisely identifying risks in steady-speed driving scenarios with minimal relative velocities. To address this, we implemented specific strategies in vehicle grouping and the quantification of vehicle-group risk.

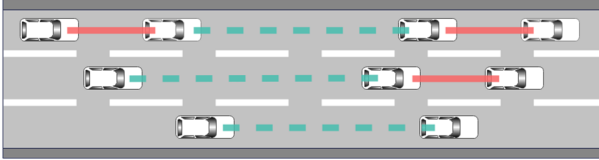
$$TTC_{i,k}(j) = \begin{cases} \frac{x_{i-1,k}(j) - x_{i,k}(j) - d_{i-1,k}}{v_{i,k}(j) - v_{i-1,k}(j)}, & v_{i,k}(j) > v_{i-1,k}(j) \\ \infty, & v_{i,k}(j) \leq v_{i-1,k}(j) \end{cases} \quad (1)$$

where $TTC_{i,k}(j)$ represents the Time-to-Collision value of the i^{th} vehicle and $i-1^{\text{th}}$ vehicle in the k^{th} vehicle group at j^{th} timestamp. $x_{i,k}(j)$ is the position of the vehicle. $d_{i,k}$ is the length of the vehicle. $v_{i,k}(j)$ is the speed of the vehicle.

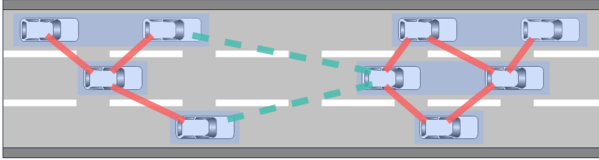
2) Vehicle-group segmentation within individual timestamps

The vehicle-group segmentation within individual timestamps involved two distinct steps: firstly, segmenting vehicle groups within a single lane, and secondly, merging these groups across adjacent lanes, as depicted in **Figure 1**.

Step 1: Vehicle-group segmentation of one lane



Step 2: Vehicle-group merging across adjacent lanes



Result: Vehicle-group segmentation within individual timestamps

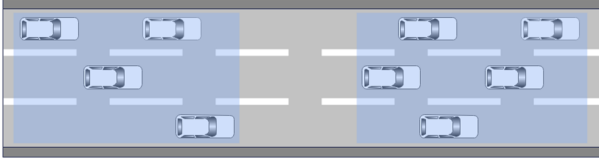


Fig. 1. Vehicle-group segmentation within individual timestamps

The first step in vehicle-group segmentation in a single lane involved calculating the TTC under adverse driving conditions to amplify the potential risk between leading and following vehicles, as outlined in **Eq. (2)** and **(3)**. This calculation simulated sudden braking behavior by setting a predefined deceleration rate and time for the leading vehicle. The braking of the leading vehicle is a critical risk factor for rear-end crashes, which constitutes the most frequent type of multi-vehicle crashes [41]. The recommended average maximum deceleration rate of $3\text{m}\cdot\text{s}^{-2}$ by ITE [42] was adopted. Accordingly, the deceleration rate was set to $-3\text{m}\cdot\text{s}^{-2}$ with a

deceleration time of 1s. If the TTC of the leading and following vehicles was smaller than a predefined TTC threshold, the two vehicles were grouped. For this study, the TTC threshold value was established at 1.5s [39, 43-45].

$$TTC'_{i,k}(j+t) = \begin{cases} \frac{x_{i-1,k}(j+t) - x_{i,k}(j+t) - d_{i-1,k}}{v_{i,k}(j+t) - v_{i-1,k}(j+t)}, & v_{i,k}(j+t) > v_{i-1,k}(j+t) \\ \infty, & v_{i,k}(j+t) \leq v_{i-1,k}(j+t) \end{cases} \quad (2)$$

where:

$$\begin{cases} v_{i-1,k}(j+t) = v_{i-1,k}(j) - a \cdot t \\ x_{i-1,k}(j+t) = x_{i-1,k}(j) + v_{i-1,k}(j) \cdot t - \frac{1}{2} a \cdot t^2 \\ v_{i,k}(j+t) = v_{i,k}(j) \\ x_{i,k}(j+t) = x_{i,k}(j) + v_{i,k}(j) \cdot t \end{cases} \quad (3)$$

where $TTC'_{i,k}(j+t)$ is the TTC calculated under adverse driving conditions. a is the absolute value of a predefined deceleration rate for the leading vehicle and t is a predefined deceleration time.

The second step involved merging vehicle groups across adjacent lanes. This approach acknowledges that crash risks arise not only from in-line driving but also from lateral interactions. Xu et al. [46] demonstrated that the risk of sideswipe crashes increased with greater speed differences between adjacent lanes. To account for the impact of adjacent-lane traffic flows on crash risks, vehicle groups across multiple lanes were merged. The standard TTC calculation, initially designed for vehicles in a single lane, was modified for adjacent vehicles. This modification entailed replacing the single-lane headway in **Eq. (1)**, denoted as $x_{i-1}(j) - x_i(j)$, with the projected headway of two adjacent vehicles on the lane line between them, represented as $x_{i-1}^p(j) - x_i^p(j)$ in **Figure 2**. This adjustment was based on the understanding that significant speed disparities or minimal projected headways between adjacent vehicles increase sideswipe crash risks. If the projected TTC between any two vehicles from different groups was smaller than a predefined TTC threshold, their respective vehicle groups were merged into one. When a vehicle group was eligible to merge with multiple groups across lanes, these groups were collectively considered as a larger vehicle group. Extensive testing set the TTC threshold to 3s [47-49].

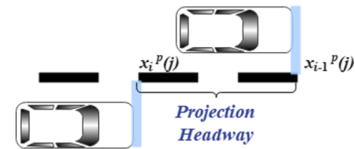


Fig. 2. Projected headway of vehicles from adjacent lanes

3) Vehicle-group matching of adjacent timestamps

After segmenting vehicle groups at individual timestamps, these groups were matched across consecutive timestamps to establish vehicle-group trajectories, as depicted in **Figure 3**. Owing to random vehicle movements, vehicle groups differed across timestamps. To streamline the matching process, two

distinct features were identified: “head vehicles” and the “composition of the vehicle group”. These features were crucial in accurately aligning vehicle groups over successive timestamps.

In each vehicle group, the leading vehicles within their respective lanes were designated as “head vehicles”. The actions of these head vehicles significantly impact the behavior of the following vehicles in the same lane. For example, Wang et al. [50] showed that the deceleration of the leading vehicle in a platoon led to a narrowing spacing between vehicles and the decrease of the overall speed of the platoon. To match vehicle groups across adjacent timestamps, a key criterion was the continuity of head vehicles. If one or more head vehicles were common between two vehicle groups in consecutive timestamps, these groups were matched accordingly, as illustrated in **Figure 3**.

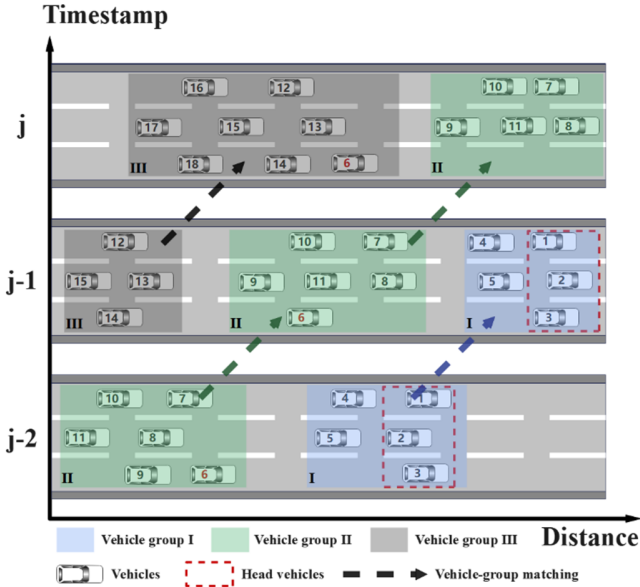


Fig. 3. Vehicle-group matching

In certain scenarios, a vehicle group could have multiple potential matches in adjacent timestamps based solely on the criterion of head vehicles. For instance, as depicted in **Figure 3**, vehicle 6, due to its slow speed, becomes the head vehicle of vehicle group III at the j^{th} timestamp. This leads to a situation where vehicle group II at the $(j-1)^{\text{th}}$ timestamp could be matched with both vehicle groups II and III at the j^{th} timestamp. To resolve such ambiguities, the “composition of the vehicle group” was employed as an additional matching criterion. When a vehicle group had several matchable counterparts, the similarity in composition between the vehicle group and its potential matches was evaluated, as detailed in **Eq. (4)**. The vehicle group with the highest similarity in composition was then selected as the most suitable match.

$$S_k(j, j+1) = \frac{i_k(j, j+1)}{n_k(j+1)} \quad (4)$$

where $S_k(j, j+1)$ represents the similarity between the k^{th}

vehicle group at the j^{th} timestamp and its corresponding matchable vehicle group at the $(j+1)^{\text{th}}$ timestamp. $i_k(j, j+1)$ denotes the number of vehicles common to both groups. $n_k(j+1)$ refers to the total number of vehicles in the matchable vehicle group at the $(j+1)^{\text{th}}$ timestamp.

B. Statistical Models

To analyze the formation of crash risks, this study employed binomial logistic regression models, examining the influence of vehicle group and road section attributes. Logistic regression, a robust classification model, offers a clear interpretation of relationships between independent and dependent variables, as outlined in **Eq. (5)**. This research focused on the impact of variables from the current timestamp on crash risk formation in the subsequent timestamp. Initially, the interval between two adjacent timestamps was set at 5 seconds. However, subsequent sections of this study explore the effects of varying time intervals (such as 2 seconds and 1 second) on the outcomes of vehicle grouping and crash risk formation analysis.

$$\log \frac{p}{1-p} = \beta_0 + \beta_1 x_1 + \beta_2 x_2 + \dots + \beta_m x_m \quad (5)$$

where p is the probability of the dependent variable equaling a case rather than a non-case. β_0 is the intercept. β_i , $i=1, 2, \dots, m$, is the coefficient of independent variable x_i .

Logistic regression models were also applied in examining the propagation of crash risks, aiming to investigate the relationship between various crash risk propagation patterns and the characteristics of vehicle-group movement. Definitions of these propagation patterns and their associated features will be detailed in the subsequent sections.

C. The quantification of vehicle-group risk

The crash risk for a vehicle group was determined as the inverse of the smallest TTC value among all pairs of leading and following vehicles within the group, as indicated in **Eq. (6)**. If the risk of a vehicle group exceeded the threshold of $1/1.5 \text{ s}^{-1}$, the vehicle group was classified as high risk.

$$Risk_k(j) = \frac{1}{\min(\{TTC_{i,k}(j) | i \in G_k(j)\})} \quad (6)$$

where $Risk_k(j)$ is the crash risk of the k^{th} vehicle group at the j^{th} timestamp. $G_k(j)$ is the k^{th} vehicle group at the j^{th} timestamp.

The computation of TTC was conducted under two scenarios: in-lane driving and during lane-changing maneuvers. For in-lane driving, **Eq. (1)** was applied directly. However, a lane-changing maneuver impacts both the original and target lanes, necessitating the creation of vehicle projections on both lanes, as shown in **Figure 4**. This method treated the lane-changing vehicle as two separate vehicles for TTC calculations. However, in some rare cases, these projected vehicles might overlap with others, leading to

negative TTC values. To address this issue, we calculated the 5th percentile of TTC values across all pairs of vehicles, road segments, and timestamps, which was found to be 1.25 seconds. When encountering negative projected TTC values, indicative of high risk, we replaced these values with 1.25 seconds to ensure that these high-risk cases were not overlooked in the analysis.

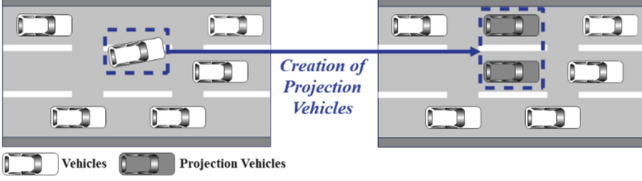


Fig. 4. The projection for lane changing vehicles

D. The definition of propagation patterns of crash risks

The propagation patterns of crash risks were categorized based on trends in the quantity of high-crash-risk occurrences. The term "quantity of high-crash-risk occurrences" was adopted as a metric to quantify the spatial aspect of risks. This measure is calculated as the count of TTC values less than 1.5 seconds within a vehicle group, as outlined in Eq. (7).

$$Q_k(j) = \text{card}(\{i | TTC_{i,k}(j) < 1.5, i \in G_k(j)\}) \quad (7)$$

where $Q_k(j)$ is the quantity of high-crash-risk occurrences.

Four propagation patterns of crash risks were identified:

- When the quantity of high risks consistently increases, the risk within the vehicle group is categorized as diffusing spatially;
- If the quantity steadily decreases, the risk is interpreted as dissipating spatially;
- A fluctuating spatial pattern is observed when the quantity of high risks alternates between increasing and decreasing;
- If the quantity remains constant, the risk is considered to be in a maintaining state.

Following the completion of vehicle-group segmentation and matching based on the dataset down-sampled to 0.2 Hz, a total of 5985 trajectories were compiled, with each spanning at least two timestamps. Figure 5 presents the distribution of these 5985 vehicle-group trajectories across various propagation patterns. Dissipation emerged as the most prevalent propagation pattern for crash risks.

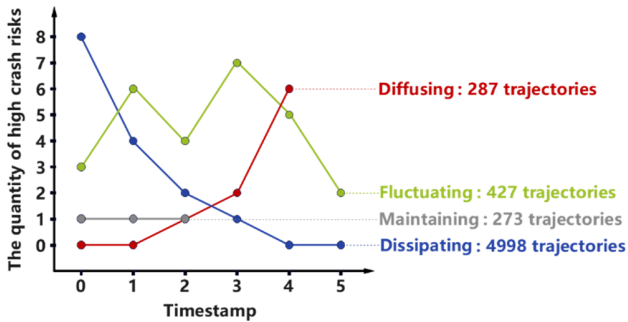


Fig. 5. Schematic diagram of different propagation patterns of

crash risks. The average duration of different patterns varied.

IV. DATA PREPARATION

A. MAGIC Dataset

This study's data were sourced from the MAGIC Dataset [36], with the locations of the road sections illustrated in Figure 6. The dataset encompasses details such as vehicle ID, type, position, speed, acceleration, timestamp, lane ID, and direction. Notably, the dataset surpasses the NGSIM and HighD datasets in terms of providing more diverse traffic states, more road section types, and longer recording durations [36], making it an invaluable asset for analyzing the formation and propagation of crash risks.

The original resolution of the dataset is 25 Hz. For the purpose of this study, it was down-sampled to intervals of 5 seconds (0.2 Hz), 2 seconds (0.5 Hz), and 1 second (1 Hz) to examine the effects of different intervals on the analysis results. Additionally, to maintain consistency in the analysis, data from only one direction of traffic were used.



Fig. 6. Location of the road section

B. Dependent Variables

In analyzing crash risk formation, the dependent variable is a binary indicator representing the risk levels of vehicle groups, defined based on the risk quantification method outlined in Section III.C. A vehicle group is classified as high risk if its risk exceeds the threshold of $1/1.5 \text{ s}^{-1}$ [39, 43-45].

For the study of crash risk propagation, the dependent variables were the propagation patterns of crash risks as detailed in Section III.D. Recognizing that dissipation is the predominant pattern, a multinomial logistic regression model was utilized, with dissipation as the reference category. This approach examines the factors causing deviations in vehicle-group risk propagation from dissipation to other patterns.

C. Independent Variables Collection

1) Candidate variables for the formation of crash risks

The independent variables selected for this analysis encompassed the motion characteristics and vehicle composition of vehicle groups, alongside their current risk levels. Additionally, geometric and traffic features of road segments were also considered, as detailed in Table I.

2) Candidate variables for the propagation of crash risks

To investigate the propagation of crash risks, features relating to the movement of vehicle groups were extracted and are outlined in Table II.

TABLE I
INDEPENDENT VARIABLES FOR THE ANALYSIS OF THE FORMATION OF CRASH RISKS

Variables	Definition	Unit
<i>max/min/avg_s</i>	the maximum (<i>max</i>), minimum (<i>min</i>), or average (<i>avg</i>) speeds (<i>s</i>) of vehicles within a vehicle group	m/s
<i>std_s</i>	the standard deviation of vehicle speeds (<i>s</i>) within a vehicle group	m/s
<i>std_a</i>	the standard deviation of vehicle accelerations (<i>a</i>) within a vehicle group	m/s ²
<i>pctg_large_veh</i>	the percentage (<i>pctg</i>) of large vehicles (<i>large_veh</i>), i.e., heavy car (10m) and bus (12m) in a vehicle group	%
<i>pctg_change_lane</i>	the percentage (<i>pctg</i>) of vehicles executing lane changes (<i>change_lane</i>) in a vehicle group	%
<i>size</i>	total number of vehicles (<i>size</i>) in a vehicle group	-
<i>risk</i>	the crash risk of the vehicle group	s ⁻¹
<i>qty_high_risk</i>	the quantity of risks higher than a threshold in a vehicle group	-
<i>segment_density</i>	the traffic density of the road segment where the vehicle group is located	veh/m
<i>segment_speed</i>	the traffic speed of the road segment where the vehicle group is located	m/s
<i>lanes</i>	the number of lanes on the road segment where the vehicle group is located	-
<i>on_ramp</i>	the count of vehicles within a 100-meter range of the on-ramp in a vehicle group	-
<i>off_ramp</i>	the count of vehicles within a 100-meter range of the off-ramp in a vehicle group	-
<i>curve</i>	the count of vehicles on a curved road section in a vehicle group	-

TABLE II
INDEPENDENT VARIABLES FOR THE ANALYSIS OF THE PROPAGATION OF CRASH RISK

Variables	Definition	Unit
<i>std/avg/cum_avg_s</i>	the standard deviation (<i>std</i>), average value (<i>avg</i>), or cumulative change (<i>cum</i>) of average speeds (<i>avg_s</i>) at all timestamps along the vehicle-group trajectory	m/s
<i>std_avg_a</i>	the standard deviation (<i>std</i>) of average accelerations (<i>avg_a</i>) at all timestamps along the vehicle-group trajectory	m/s ²
<i>std/avg/cum_size</i>	the standard deviation (<i>std</i>), average value (<i>avg</i>), or cumulative change (<i>cum</i>) of the number of vehicles in the vehicle group at all timestamps	Veh
<i>avg/sum_change_lane</i>	the average (<i>avg</i>) or total (<i>sum</i>) number of vehicles changing lanes in the vehicle group at all timestamps	Veh
<i>sum_large_veh</i>	the total count (<i>sum</i>) of large vehicles (<i>large_veh</i>), i.e., heavy car (10m) and bus (12m), along the vehicle-group trajectory	Veh
<i>sum_on_ramp</i>	the total count (<i>sum</i>) of vehicles within a 100-meter range of the on-ramp (<i>on_ramp</i>) along the vehicle-group trajectory	Veh
<i>sum_off_ramp</i>	the total count (<i>sum</i>) of vehicles within a 100-meter range of the off-ramp (<i>off_ramp</i>) along the vehicle-group trajectory	Veh
<i>timespan_high_risk</i>	the timespan (<i>timespan</i>) when the vehicle group is under high risk (<i>high_risk</i>)	s
<i>ini/max/avg_risk</i>	the initial (<i>ini</i>), maximal (<i>max</i>), or average (<i>avg</i>) value of the crash risks (<i>risk</i>) along the vehicle-group trajectory	s ⁻¹

V. RESULTS

A. Model Estimation for the Formation of Crash Risks

Three models were developed to analyze crash risk formation with different prediction intervals (5 seconds, 2 seconds, and 1 second). The dependent variable in these models is the risk level of vehicle groups, with independent variables detailed in **Table I**. Prior to modeling, the data underwent several preprocessing steps: outlier handling, feature discretization, and normalization. A significant challenge was the dataset's imbalance (non-high-risk to high-risk case ratio exceeding 10:1), potentially impacting model accuracy. To address this, a down-sampling method was applied to adjust the ratio to 4:1, aligning with practices in

previous studies [51, 52]. Furthermore, to ensure comparability across models with varying predictive intervals, the data volumes for the three datasets were equalized to match the smallest dataset. The datasets were then randomly divided into training and validation sets in a 70:30 ratio.

The variable selection process began by assessing the significance of each variable to the dependent variable. Insignificant variables were subsequently eliminated. This was followed by correlation tests to identify highly correlated variables (with coefficients exceeding 0.4). In cases of high correlation, the variable yielding a lower Akaike Information Criterion (AIC) was retained. Next, backward regression, guided by the AIC [53] was employed for further variable selection. Lastly, the Variance Inflation Factor (VIF) was utilized to evaluate multicollinearity among variables. If the

VIF for any two variables exceeded 5, the one with the lower AIC value was chosen.

The results for the cases with 5-second, 2-second, and 1-second intervals are presented in **Tables III(a)**, **III(b)**, and **III(c)**, respectively.

The results in **Table III** indicate that the model's predictive performance is enhanced with shorter prediction time intervals, evidenced by an increase in the AUC value from 0.761 to 0.906 as the interval decreases. This suggests that more recent information is crucial for accurate risk prediction, a trend likely to continue with future advancements in V2X communication and computational capabilities.

In the vehicle-group risk formation analysis, the variables identified using 2-second and 1-second intervals are identical, and encompassing those from the 5-second interval. This consistency underscores the models' reliability and robustness.

Key findings include the impact of a high percentage of large vehicles (*pctg_large_veh*) and frequent lane changes (*pctg_change_lane*) within a vehicle group on increasing crash risk. The slower speeds of large vehicles and the threat posed by their size can induce erratic driving behaviors in surrounding vehicles, such as overtaking or changing lanes. Their inferior braking capabilities and longer stopping distances further contribute to risk. Lane-changing behaviors of a vehicle on highways requires precise timing and spatial awareness, or they might result in unsafe relative positions and speeds between the vehicle and other vehicles in the target lanes.

The study also highlights the significance of motion variables such as the standard deviation of vehicle speeds and accelerations in a vehicle group (*std_s*, *std_a*). They reflect the complexity of vehicle behaviors, with greater complexity correlating with higher crash likelihood.

Risk-related features of vehicle groups, like the current risk value (*risk*) and the quantity of high-risk occurrences (*qty_high_risk*), are also crucial indicators. These findings suggest that vehicle groups already at high risk are likely to maintain this status.

Additionally, higher traffic density on a road segment (*segment_density*) typically indicates congestion, reducing vehicle spacing and increasing crash probability.

Road segment geometry also plays a significant role. The merging traffic from on-ramps (*on_ramp*) might disrupts the flow on the main road and elevates crash risk. Driving on curves (*curve*) can lead to increased crash likelihood due to factors like the centripetal force, reduced visibility, and decreased stability. While more lanes on a road segment (*lanes*) provide greater maneuvering space for vehicles, they also enable riskier behaviors such as overtaking and lane changing.

TABLE III
MODEL RESULTS FOR THE FORMATION OF CRASH RISKS

(a) Prediction Time Interval: 5s				
Variables	Coef.	Std. Error	Z value	P value
<i>on_ramp</i>	5.165	0.593	8.712	<0.001
<i>segment_density</i>	1.742	0.063	27.442	<0.001
<i>pctg_change_lane</i>	1.098	0.099	11.077	<0.001

<i>pctg_large_veh</i>	0.991	0.327	3.028	<0.001
<i>risk</i>	0.785	0.054	14.616	<0.001
<i>std_s</i>	0.618	0.065	9.456	<0.001
<i>std_a</i>	0.414	0.066	6.229	<0.001
<i>lanes</i>	0.224	0.044	5.098	<0.001
(intercept)	-3.283	0.049	-66.913	<0.001
	AUC	TPR	TNR	ACC
Training	0.761	0.655	0.743	0.726
Validation	0.761	0.722	0.675	0.694

(b) Prediction Time Interval: 2s				
Variables	Coef.	Std. Error	Z value	P value
<i>curve</i>	3.358	0.579	5.799	<0.001
<i>risk</i>	1.694	0.068	24.801	<0.001
<i>pctg_change_lane</i>	1.293	0.103	12.608	<0.001
<i>pctg_large_veh</i>	1.249	0.340	3.677	0.002
<i>min_s</i>	-0.761	0.120	-6.348	<0.001
<i>segment_density</i>	0.730	0.117	6.250	<0.001
<i>std_s</i>	0.648	0.068	9.571	<0.001
<i>std_a</i>	0.505	0.068	7.412	<0.001
<i>qty_high_risk</i>	0.486	0.096	5.037	<0.001
<i>lanes</i>	0.318	0.050	6.404	<0.001
(intercept)	-2.892	0.118	-24.498	<0.001
	AUC	TPR	TNR	ACC
Training	0.842	0.750	0.793	0.784
Validation	0.831	0.713	0.822	0.800

(c) Prediction Time Interval: 1s				
Variables	Coef.	Std. Error	Z value	P value
<i>risk</i>	2.349	0.075	31.413	<0.001
<i>curve</i>	2.313	0.521	4.436	<0.001
<i>pctg_change_lane</i>	1.594	0.119	13.404	<0.001
<i>qty_high_risk</i>	1.532	0.141	10.888	<0.001
<i>pctg_large_veh</i>	1.047	0.419	2.499	0.012
<i>std_a</i>	0.995	0.079	12.662	<0.001
<i>min_s</i>	-0.837	0.132	-6.341	<0.001
<i>std_s</i>	0.519	0.082	6.319	<0.001
<i>segment_density</i>	0.473	0.128	3.697	<0.001
<i>lanes</i>	0.152	0.058	2.634	0.008
	AUC	TPR	TNR	ACC
Training	0.906	0.812	0.870	0.858
Validation	0.906	0.832	0.850	0.847

B. Model Performance Using Alternative Classifiers

Logistic Regression (LR) is a robust and interpretable classifier, which can be used to explain the vehicle-group risk prediction results. However, as a fundamentally linear model, its effectiveness is limited under certain conditions. Therefore, this study evaluated four classifiers showing great performance on crash risk discrimination: Decision Tree (DT) [54], Random Forest (RF) [20, 55], Support Vector Machine (SVM) [56, 57], and Neural Network (NN) [58, 59], using the same significant variables identified by LR to predict vehicle-group risk. The SVM employed an RBF kernel, and the NN was structured with three fully-connected hidden layers containing 10, 20, and 10 neurons, respectively. We used

inference latency as a measure of the computational cost for each model. This latency was calculated as an average over three runs on the validation dataset comprising 10,759 records, processed using an Intel i9-13900KF CPU. Comparative analysis of model performance and computational costs are presented in **TABLE IV** and **TABLE V**. Notably, the RF classifier showed enhanced performance coupled with a relatively low inference latency. It is also found that when the prediction interval is 1 second, the classifiers exhibited similar performance. The results underscore the importance of data quality in producing accurate predictions.

TABLE IV
MODEL PERFORMANCE OVER DIFFERENT PREDICTION TIME INTERVALS AND CLASSIFIERS

AUC(Train/Test)	1s	2s	5s
LR	0.906/0.906	0.842/0.831	0.761/0.761
DT	0.904/0.901	0.846/0.828	0.755/0.749
SVM	0.893/0.891	0.819/0.811	0.677/0.672
RF	0.915/0.910	0.856/0.842	0.772/0.763
NN	0.914/0.912	0.853/0.841	0.771/0.766

TABLE V
COMPUTATIONAL COST OVER DIFFERENT PREDICTION TIME INTERVALS AND CLASSIFIERS

Inference Latency (millisecond)	1s	2s	5s
LR	0.003	0.003	0.003
DT	0.739	0.759	0.766
SVM	1931.041	2333.043	2355.121
RF	6.691	9.146	11.238
NN	60.852	61.228	59.039

C. Model Performance Using Adaptive TTC Threshold

Previous research often used a constant TTC threshold to identify high crash risk [39, 43-45, 47-49]. This study utilized thresholds of 1.5 seconds for in-lane vehicle grouping and 3 seconds for adjacent lanes. When assessing vehicle group risk, a 1.5-second threshold (equivalent to a vehicle-group risk of $1/1.5 \text{ s}^{-1}$) was employed to categorize high-risk vehicle groups. However, the TTC threshold might be varying under different traffic environments (e.g., density). For instance, model results in **Section V.A** indicate that higher road segment density correlates with increased crash risk, attributed to decreased spacing between vehicles and thus lower TTC values. However, according to the Fundamental Diagram [60-62], higher density typically accompanies lower speeds. In such scenarios, despite lower TTC values, the actual probability of a crash might not be as high as suggested, implying the need for a lower TTC threshold (implying a higher vehicle-group risk threshold). Conversely, in lower density conditions, larger TTC thresholds might be more appropriate.

Recent studies in the field have introduced the concept of adaptive TTC thresholds, tailoring them to specific driver characteristics, environmental conditions [63], and types of

leading vehicles [49]. In this research, adaptive TTC thresholds were established based on the traffic density of road segments. However, it's important to acknowledge that, due to the absence of actual accident data in the dataset, the efficacy and appropriateness of the adaptive TTC thresholds remain unvalidated.

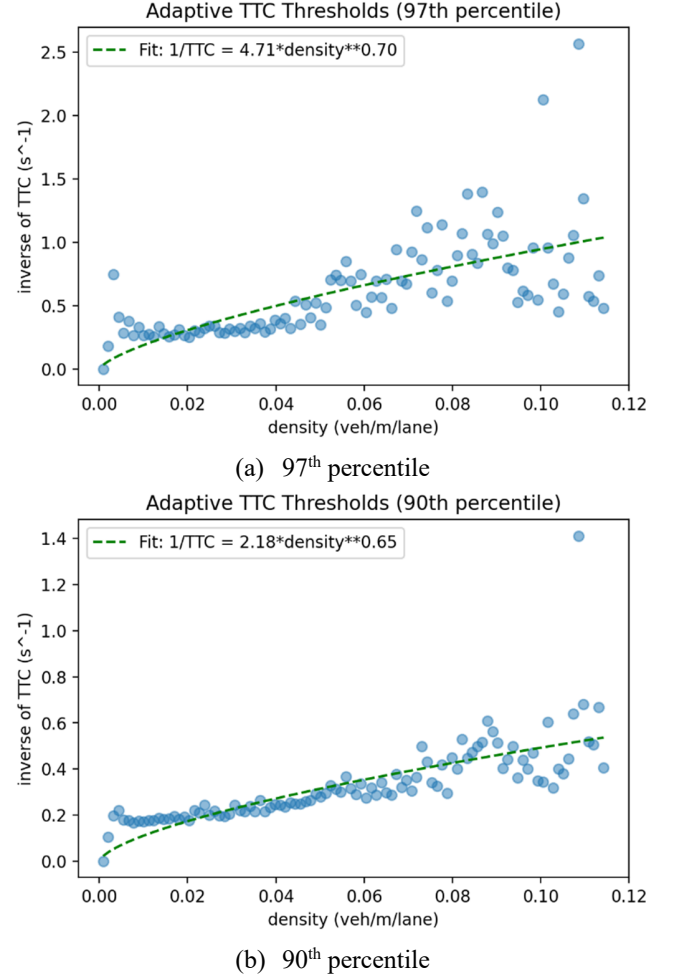


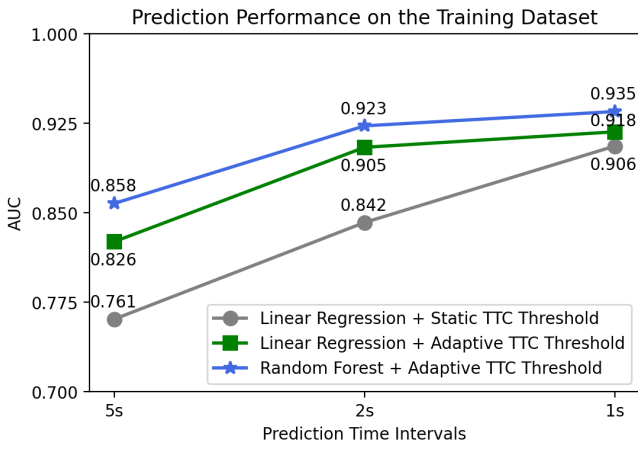
Fig. 7. Adaptive TTC thresholds

To derive adaptive TTC thresholds, the dataset was down-sampled to 0.5 Hz (corresponding to a 2-second interval). First, the average potential risk (inverse of TTC) among all vehicle pairs on road segments across different traffic densities was calculated. Subsequently, the density range was segmented into 100 equal intervals. For enhanced discrimination of high-risk events and effective vehicle-group segmentation, the 97th and 90th percentile values of inverse TTC were computed within corresponding density intervals. Two functions mapping densities to inverse TTC values were then developed based on these percentiles, as illustrated in **Figure 7**. **Figure 7(a)** shows the density- inverse TTC mapping under 97th percentile and was used for in-lane vehicle grouping. **Figure 7(b)** shows the density-inverse TTC mapping under 90th percentile and was applied for merging vehicle groups in adjacent lanes.

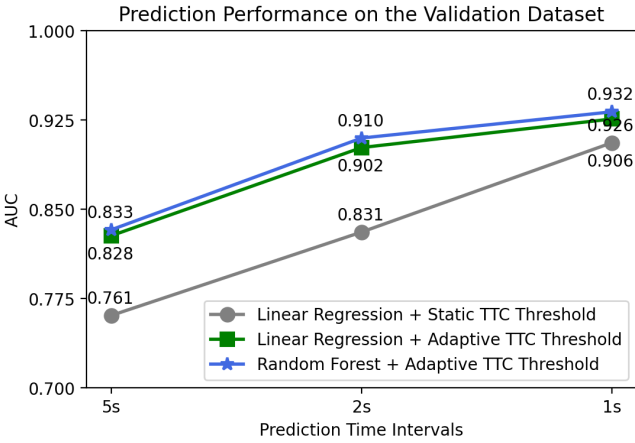
A comparison was made between the sizes of vehicle groups formed using static and adaptive TTC thresholds, as detailed in **Table VI**. The introduction of adaptive TTC thresholds resulted in more controlled vehicle group sizes. Specifically, the maximum number of vehicles in a group reduced from over 100 to under 90, with smaller standard deviations.

TABLE VI
COMPARISON OF VEHICLE-GROUP SIZES

Prediction Time Interval: 5s/2s/1s	Static TTC Threshold	Adaptive TTC Threshold
Max	101/105/114	92/89/92
Std	4.82/4.83/4.84	4.46/4.47/4.46



(a) Training dataset



(b) Validation dataset

Fig. 8. Model performance using adaptive TTC thresholds

Model performance using Logistic Regression and Random Forest is depicted in **Figure 8**. The introduction of adaptive TTC thresholds significantly enhanced model efficacy, particularly for longer predictive time intervals. The AUC value increased by around 0.065 for the 5-second interval and the 2-second interval. Utilizing Random Forest, the AUC value reached more than 0.93 for the 1-second interval. These results indicate that adaptive TTC thresholds potentially

improve the prediction of vehicle-group risks.

D. Model estimation for the propagation of crash risks

A multinomial logistic regression model was utilized to examine crash risk propagation, using dissipation as the reference pattern (i.e., labeled as 0). The independent variables are detailed in **Table II**. Adhering to similar data processing steps as in **Section V.A**, but excluding down-sampling, the findings are presented in **Table VII**.

In this study, since the data was normalized, we could gauge the impact of variables through the absolute values of their coefficients. Following this principle, two variables were identified as particularly influential in determining crash risk propagation patterns: the duration of high-risk status (*timespan_high_risk*) and the cumulative change in the size of vehicle groups (*cum_size*). The positive coefficients indicate that extended high-risk periods and increases in vehicle-group size are associated with adverse propagation patterns, notably diffusion and fluctuation. Such spatial risk diffusion and fluctuation may trigger deceleration and evasive maneuvers, leading to the merging of vehicle groups. Given that a vehicle group is a cluster of closely related vehicles, risk diffusion can create a domino effect. The size of the vehicle group influences the extent of risk propagation, with larger groups fostering an environment conducive to further risk diffusion and fluctuation.

Furthermore, an increase in both the standard deviation and the average of vehicle speeds within a group over its trajectory (*std_avg_s*, *avg_avg_s*) appears to contribute to risk dissipation, as indicated by their negative coefficients. Elevated deviation and average speed within a vehicle group typically signify a smoother traffic flow, which is instrumental in mitigating the spread of crash risks.

The negative coefficient for the initial crash risk value (*ini_risk*) suggests that the dissipation pattern of risks is more likely to start from a higher initial risk compared to diffusion and maintaining patterns. Risk diffusion can resemble a domino effect, where the crash risk in a vehicle group may increase due to the cumulative effect of drivers' reaction times. This diffusion process may reach a peak and then begin to dissipate once the risk reaches a certain threshold.

Additionally, an increase in the average number of lane-changing vehicles within a group (*avg_change_lane*) seems to facilitate risk diffusion. Lane-changing, typically executed by drivers to access faster lanes and improve travel efficiency, can disrupt the traffic flow in the target lane, leading to risk diffusion and enhanced crash potential.

Lastly, the presence of a larger number of heavy vehicles in a vehicle group's movement (*num_large_veh*) is found to be positively correlated with risk fluctuation as opposed to dissipation. Heavy vehicles, characterized by their larger mass, slower acceleration, and reduced braking efficiency, require more time to adjust their speed, contributing to notable disruptions in traffic flow and greater fluctuations in crash risks.

TABLE VII
MODEL RESULTS FOR THE PROPAGATION OF CRASH RISKS PATTERNS

	Variables	Coefficient	Standard Error	Z value	P value
Maintaining	<i>std_avg_s</i>	-6.614	0.919	-7.199	<0.001
	<i>avg_avg_s</i>	0.026	0.338	0.078	0.938
	<i>cum_size</i>	13.056	1.488	8.776	<0.001
	<i>avg_change_lane</i>	-0.067	1.059	-0.064	0.949
	<i>num_off_ramp</i>	-2.839	0.937	-3.029	0.002
	<i>num_large_veh</i>	0.384	0.484	0.793	0.428
	<i>timespan_high_risk</i>	29.711	1.338	22.209	<0.001
	<i>ini_risk</i>	-9.151	3.913	-2.339	0.019
	<i>(intercept)</i>	-10.418	0.837	-12.452	<0.001
Diffusion	<i>std_avg_s</i>	-6.004	1.035	-5.800	<0.001
	<i>avg_avg_s</i>	-1.039	0.407	-2.553	0.011
	<i>cum_size</i>	24.839	1.643	15.120	<0.001
	<i>avg_change_lane</i>	2.522	0.819	3.077	0.002
	<i>num_off_ramp</i>	-1.293	0.730	-1.771	0.077
	<i>num_large_veh</i>	0.208	0.492	0.422	0.673
	<i>timespan_high_risk</i>	28.028	1.460	19.200	<0.001
	<i>ini_risk</i>	-5.643	2.484	-2.272	0.023
	<i>(intercept)</i>	-16.968	0.948	-17.902	<0.001
Fluctuation	<i>std_avg_s</i>	0.990	0.724	1.367	0.172
	<i>avg_avg_s</i>	-3.787	0.674	-5.615	<0.001
	<i>cum_size</i>	9.200	1.153	7.982	<0.001
	<i>avg_change_lane</i>	1.237	0.751	1.648	0.099
	<i>num_off_ramp</i>	0.828	0.525	1.579	0.114
	<i>num_large_veh</i>	1.801	0.413	4.356	<0.001
	<i>timespan_high_risk</i>	38.984	1.406	27.719	<0.001
	<i>ini_risk</i>	-2.221	1.439	-1.544	0.123
	<i>(intercept)</i>	-9.813	0.675	-14.528	<0.001

*Reference Pattern: Dissipation (labeled as 0)

VI. DISCUSSION AND CONCLUSIONS

Previous studies on predicting crash risks for expressways primarily associated crash occurrences with traffic parameters or the geometric features of road segments. However, these studies could not fully account for the impact of vehicles' past driving states and their interactions with nearby vehicles on future risks statuses. Thus, based on a high-fidelity trajectory dataset, this study constructed trajectories of vehicle groups to capture these kinds of impact and analyze the formation and propagation mechanisms of crash risks.

The construction of vehicle group trajectories involved two key stages: segmentation within individual timestamps and subsequent matching. Initially, vehicle groups were segmented at each timestamp based on the potential risks between vehicles, determined using TTC values. If the TTC indicated a sufficient risk, vehicles were classified as part of the same group. To form continuous trajectories, two primary features – the identity of head vehicles and the overall composition of each vehicle group – were utilized. These features facilitated the matching of vehicle groups across consecutive timestamps.

The risk formation analysis revealed several key factors elevating crash likelihood: a high proportion of large vehicles and frequent lane changes within a vehicle group, complex

vehicle behaviors, historical states of high risk in vehicle groups, and specific road segment geometries, including the presence of on-ramps, curved segments, and the number of lanes. Additionally, high traffic density on road segments was also identified as a risk enhancer. The study performed a sensitivity analysis encompassing different classifiers, prediction time intervals, and adaptive TTC thresholds. A notable increase was observed in the AUC value for risk prediction as the prediction time interval shortened from 5 seconds to 1 second, rising from 0.761 to 0.906. This trend underscores the significance of utilizing more recent information for precise vehicle-group risk prediction. With the incorporation of the Random-Forest Classifier, coupled with adaptive TTC thresholds, the AUC value exhibited further improvement, surpassing 0.910 and 0.930, respectively.

In terms of risk propagation, the study found that extended periods of high-risk status, an increase in vehicle-group size, and frequent lane changes contribute to negative propagation patterns, specifically risk diffusion and fluctuation. Conversely, a high standard deviation and average speed within a vehicle group, as well as a high initial crash risk value at the start of a vehicle-group trajectory, are associated with the spatial dissipation of crash risks. These findings highlight the complex dynamics of risk propagation in vehicle groups.

The findings of this study are instrumental in determining crash risks for moving vehicle groups, providing crucial insights for developing crash-avoidance strategies in Connected and Autonomous Vehicles (CAVs). Through communication between vehicles and with roadside units, CAVs can access traffic and environmental data to assess the crash risks of vehicle groups. Upon detecting high crash risks, group-level risk-avoidance strategies can be deployed. These may include maintaining uniform speeds and accelerations within a vehicle group and coordinating lane-changing maneuvers. Additionally, to curb the diffusion and fluctuation propagation of crash risks, strategies could involve controlling vehicles to prevent merging with other vehicle groups, thereby enhancing overall traffic safety.

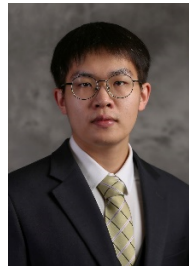
There are some limitations in this study. One significant constraint is the absence of weather data in the MAGIC dataset, leading to the exclusion of weather-related variables that are known to considerably influence crash risks. Given that risk precursors can vary under different weather conditions, future research could enhance the current findings by integrating weather information. Furthermore, while microscopic features of vehicles play a vital role in understanding crash-risk mechanisms, the features in this study were determined empirically, potentially overlooking some critical factors. Future research could employ advanced techniques, such as deep learning, to derive more comprehensive vehicle features, thereby facilitating a more profound understanding of crash risk dynamics.

REFERENCES

- [1] M. Hasan, S. Mohan, T. Shimizu, and H. Lu, "Securing vehicle-to-everything (V2X) communication platforms," *IEEE Trans. Intell. Veh.*, vol. 5, no. 4, pp. 693-713, 2020.
- [2] W. Ma, Z. He, L. Wang, M. Abdel-Aty, and C. Yu, "Active traffic management strategies for expressways based on crash risk prediction of moving vehicle groups," *Accid. Anal. Prev.*, vol. 163, p. 106421, Dec 2021, doi: 10.1016/j.aap.2021.106421.
- [3] L. Wang, M. Abdel-Aty, Q. Shi, and J. Park, "Real-time crash prediction for expressway weaving segments," *Transp. Res. Part C: Emerg. Technol.*, vol. 61, pp. 1-10, 2015, doi: 10.1016/j.trc.2015.10.008.
- [4] R. Yu, X. Wang, K. Yang, and M. Abdel-Aty, "Crash risk analysis for Shanghai urban expressways: A Bayesian semi-parametric modeling approach," *Accid. Anal. Prev.*, vol. 95, pp. 495-502, 2016.
- [5] K. Yang, X. Wang, and R. Yu, "A Bayesian dynamic updating approach for urban expressway real-time crash risk evaluation," *Transp. Res. Part C: Emerg. Technol.*, vol. 96, pp. 192-207, 2018, doi: 10.1016/j.trc.2018.09.020.
- [6] Z. Cheng, J. Yuan, B. Yu, J. Lu, and Y. Zhao, "Crash Risks Evaluation of Urban Expressways: A Case Study in Shanghai," *IEEE Trans. Intell. Transp. Syst.*, vol. 23, no. 9, pp. 15329-15339, 2022, doi: 10.1109/tits.2022.3140345.
- [7] J. Nidamanuri, C. Nibhanupudi, R. Assfalg, and H. Venkataraman, "A Progressive Review: Emerging Technologies for ADAS Driven Solutions," *IEEE Trans. Intell. Veh.*, vol. 7, no. 2, pp. 326-341, 2022, doi: 10.1109/TIV.2021.3122898.
- [8] J. Yoo and R. Langari, "A predictive perception model and control strategy for collision-free autonomous driving," *IEEE Trans. Intell. Transp. Syst.*, vol. 20, no. 11, pp. 4078-4091, 2018.
- [9] S. Levine and V. Koltun, "Continuous inverse optimal control with locally optimal examples," *arXiv preprint arXiv:1206.4617*, 2012.
- [10] J. Kim and D. Kum, "Collision risk assessment algorithm via lane-based probabilistic motion prediction of surrounding vehicles," *IEEE Trans. Intell. Transp. Syst.*, vol. 19, no. 9, pp. 2965-2976, 2017.
- [11] Y. Xia, Z. Qu, Z. Sun, and Z. Li, "A human-like model to understand surrounding vehicles' lane changing intentions for autonomous driving," *IEEE Trans. VT.*, vol. 70, no. 5, pp. 4178-4189, 2021.
- [12] W.-X. Zhu and H. M. Zhang, "Analysis of mixed traffic flow with human-driving and autonomous cars based on car-following model," *Physica A*, vol. 496, pp. 274-285, 2018.
- [13] L. Wang, M. Abdel-Aty, W. Ma, J. Hu, and H. Zhong, "Quasi-vehicle-trajectory-based real-time safety analysis for expressways," *Transp. Res. Part C: Emerg. Technol.*, vol. 103, pp. 30-38, 2019, doi: 10.1016/j.trc.2019.04.003.
- [14] N. Arbabzadeh and M. Jafari, "A data-driven approach for driving safety risk prediction using driver behavior and roadway information data," *IEEE Trans. Intell. Transp. Syst.*, vol. 19, no. 2, pp. 446-460, 2017.
- [15] Y. Rong, H. Wen, and S. Zhao, "Study on driving risk measurement for two-lane freeway vehicle group," *J. Chongqing Jiaotong Univ.*, vol. 38, pp. 95-100+121, 2019. (in Chinese)
- [16] J. Liang, W. Zhang, M. He, L. Chen, X. Xiong, and T. Cai, "A blocking efficiency evaluation method for chains of road traffic incident in IOV environment," *J. Highway Transp. Res. Dev.*, vol. 31, no. 04, pp. 211-221, 2018, doi: 10.19721/j.cnki.1001-7372.2018.04.025. (in Chinese)
- [17] X. Li, J. Liang, and T. Hao, "A Method for Quantitatively Analyzing Risks Associated with the Operation of Urban Buses Considering Chained Conflicts," *J. Transp. Info. Saf.*, vol. 40, pp. 19-29, 2022. (in Chinese)
- [18] R. Yu, M. Quddus, X. Wang, and K. Yang, "Impact of data aggregation approaches on the relationships between operating speed and traffic safety," *Accid. Anal. Prev.*, vol. 120, pp. 304-310, 2018.
- [19] M. Abdel-Aty, N. Uddin, and A. Pande, "Split models for predicting multivehicle crashes during high-speed and low-speed operating conditions on freeways," *Transp. Res. Rec.*, vol. 1908, no. 1, pp. 51-58, 2005.

- [20] A. Pande, A. Das, M. A. Abdel-Aty, and H. Hassan, "Real-time crash risk estimation: Are all freeways created equal?" in *90th TRB Annual Meeting*, Washington D.C.
- [21] M. Liu and Y. Chen, "Predicting Real-Time Crash Risk for Urban Expressways in China," *Math. Probl. Eng.*, vol. 2017, p. 6263726, 2017/01/30 2017, doi: 10.1155/2017/6263726.
- [22] K. Yang, R. Yu, X. Wang, M. Quddus, and L. Xue, "How to determine an optimal threshold to classify real-time crash-prone traffic conditions?," *Accid. Anal. Prev.*, vol. 117, pp. 250-261, 2018.
- [23] M. Hossain, M. Abdel-Aty, M. A. Quddus, Y. Muromachi, and S. N. Sadeek, "Real-time crash prediction models: State-of-the-art, design pathways and ubiquitous requirements," *Accid. Anal. Prev.*, vol. 124, pp. 66-84, Mar 2019, doi: 10.1016/j.aap.2018.12.022.
- [24] J. You, J. Wang, and J. Guo, "Real-time crash prediction on freeways using data mining and emerging techniques," *J. Mod. Transp.*, vol. 25, no. 2, pp. 116-123, 2017/06/01 2017, doi: 10.1007/s40534-017-0129-7.
- [25] J. Wang, Y. Kong, and T. Fu, "Expressway crash risk prediction using back propagation neural network: A brief investigation on safety resilience," *Accid. Anal. Prev.*, vol. 124, pp. 180-192, 2019/03/01/ 2019, doi: <https://doi.org/10.1016/j.aap.2019.01.007>.
- [26] C. Katrakazas, M. Quddus, and W.-H. Chen, "A new integrated collision risk assessment methodology for autonomous vehicles," *Accid. Anal. Prev.*, vol. 127, pp. 61-79, 2019/06/01/ 2019, doi: <https://doi.org/10.1016/j.aap.2019.01.029>.
- [27] V. Mahajan, C. Katrakazas, and C. Antoniou, "Crash risk estimation due to lane changing: A data-driven approach using naturalistic data," *IEEE Trans. Intell. Transp. Syst.*, vol. 23, no. 4, pp. 3756-3765, 2020.
- [28] R. Yu, L. Han, and H. Zhang, "Trajectory data based freeway high-risk events prediction and its influencing factors analyses," *Accid. Anal. Prev.*, vol. 154, p. 106085, 2021.
- [29] O. Zheng, M. Abdel-Aty, L. Yue, A. Abdelraouf, Z. Wang, and N. Mahmoud, "CitySim: A drone-based vehicle trajectory dataset for safety oriented research and digital twins," *arXiv preprint arXiv:2208.11036*, 2022.
- [30] L. Wang, Q. Shi, and M. Abdel-Aty, "Predicting crashes on expressway ramps with real-time traffic and weather data," *Transp. Res. Rec.*, vol. 2514, no. 1, pp. 32-38, 2015.
- [31] Y. Wu, M. Abdel-Aty, and J. Lee, "Crash risk analysis during fog conditions using real-time traffic data," *Accid. Anal. Prev.*, vol. 114, pp. 4-11, May 2018, doi: 10.1016/j.aap.2017.05.004.
- [32] M. Guo *et al.*, "A study of freeway crash risk prediction and interpretation based on risky driving behavior and traffic flow data," *Accid. Anal. Prev.*, vol. 160, p. 106328, 2021/09/01/ 2021, doi: <https://doi.org/10.1016/j.aap.2021.106328>.
- [33] J. Bao, P. Liu, and S. V. Ukkusuri, "A spatiotemporal deep learning approach for citywide short-term crash risk prediction with multi-source data," *Accid. Anal. Prev.*, vol. 122, pp. 239-254, 2019/01/01/ 2019, doi: <https://doi.org/10.1016/j.aap.2018.10.015>.
- [34] P. Li, M. Abdel-Aty, and J. Yuan, "Real-time crash risk prediction on arterials based on LSTM-CNN," *Accid. Anal. Prev.*, vol. 135, p. 105371, 2020/02/01/ 2020, doi: <https://doi.org/10.1016/j.aap.2019.105371>.
- [35] B. Dimitrijevic, S. D. Khales, R. Asadi, and J. Lee, "Short-Term Segment-Level Crash Risk Prediction Using Advanced Data Modeling with Proactive and Reactive Crash Data," *Appl. Sci.*, vol. 12, no. 2, doi: 10.3390/app12020856.
- [36] W. Ma, H. Zhong, L. Wang, L. Jiang, and M. Abdel-Aty, "MAGIC Dataset: Multiple Conditions Unmanned Aerial Vehicle Group-Based High-Fidelity Comprehensive Vehicle Trajectory Dataset," *Transp. Res. Rec.*, vol. 2676, no. 5, pp. 793-805, 2022/05/01 2022, doi: 10.1177/03611981211070549.
- [37] L. Wang, L. Zou, M. Abdel-Aty, and W. Ma, "Expressway rear-end crash risk evolution mechanism analysis under different traffic states," *Transp. B*, vol. 11, no. 1, pp. 510-527, 2022, doi: 10.1080/21680566.2022.2101565.
- [38] J. C. Hayward, "Near miss determination through use of a scale of danger," in *50th TRB Annual Meeting*, ashington D.C.
- [39] C. Wang, Y. Xie, H. Huang, and P. Liu, "A review of surrogate safety measures and their applications in connected and automated vehicles safety modeling," *Accid. Anal. Prev.*, vol. 157, p. 106157, 2021/07/01/ 2021, doi: <https://doi.org/10.1016/j.aap.2021.106157>.
- [40] K. Ozbay, H. Yang, B. Bartin, and S. Mudigonda, "Derivation and validation of new simulation-based surrogate safety measure," *Transp. Res. Rec.*, vol. 2083, no. 1, pp. 105-113, 2008.
- [41] E. Dabbour, O. Dabbour, and A. A. Martinez, "Temporal stability of the factors related to the severity of drivers' injuries in rear-end collisions," *Accid. Anal. Prev.*, vol. 142, p. 105562, 2020/07/01/ 2020, doi: <https://doi.org/10.1016/j.aap.2020.105562>.
- [42] ITE, Ed. *Traffic Engineering Handbook*. Institute of Transportation Engineers, 2009.
- [43] J. Hang, X. Yan, X. Li, K. Duan, J. Yang, and Q. Xue, "An improved automated braking system for rear-end collisions: A study based on a driving simulator experiment," *J. Safety Res.*, vol. 80, pp. 416-427, 2022.
- [44] H. Zhang, J. Sun, and Y. Tian, "Accelerated Safety Testing for Highly Automated Vehicles: Application and Capability Comparison of Surrogate Models," *IEEE Trans. Intell. Veh.*, pp. 1-10, 2023, doi: 10.1109/TIV.2023.3319158.
- [45] A. Svensson, *A method for analysing the traffic process in a safety perspective*. Lund Institute of Technology Sweden, 1998.

- [46] C. Xu, Y. Wang, P. Liu, W. Wang, and J. Bao, "Quantitative risk assessment of freeway crash casualty using high-resolution traffic data," *Reliab. Eng. Syst. Saf.*, vol. 169, pp. 299-311, 2018/01/01/ 2018, doi: <https://doi.org/10.1016/j.ress.2017.09.005>.
- [47] S. Hirst and R. Graham, "The format and perception of collision warnings," in ESIDI, Y.I. Noy, Ed. Mahwah, NJ, USA: Lawrence Erlbaum Associates, 1997, pp. 203-219.
- [48] T. L. Brown, J. D. Lee, and D. V. McGehee, "Human performance models and rear-end collision avoidance algorithms," *Hum. Factors*, vol. 43, no. 3, pp. 462-482, 2001.
- [49] S. Das and A. K. Maurya, "Defining Time-to-Collision Thresholds by the Type of Lead Vehicle in Non-Lane-Based Traffic Environments," *IEEE Trans. Intell. Transp. Syst.*, vol. 21, no. 12, pp. 4972-4982, 2020, doi: 10.1109/tits.2019.2946001.
- [50] K. Wang, H. Liu, J. Zeng, C. Niu, F. Cao, and J. Ji, "Analysis and Prevention of Chain Collision in Traditional and Connected Vehicular Platoon," in *2020 4th CVCI*, 2020, pp. 726-730, doi: 10.1109/CVCI51460.2020.9338496.
- [51] S. Roshandel, Z. Zheng, and S. Washington, "Impact of real-time traffic characteristics on freeway crash occurrence: systematic review and meta-analysis," *Accid. Anal. Prev.*, vol. 79, pp. 198-211, Jun 2015, doi: 10.1016/j.aap.2015.03.013.
- [52] Z. Zheng, S. Ahn, and C. M. Monsere, "Impact of traffic oscillations on freeway crash occurrences," *Accid. Anal. Prev.*, Article vol. 42, no. 2, pp. 626-636, Mar 2010, doi: 10.1016/j.aap.2009.10.009.
- [53] H. Akaike, "Information theory and an extension of the maximum likelihood principle," in *2nd Intl. Symposium Info. Theory*, 1973: Akademia Kiado, pp. 267-281.
- [54] H. Park, A. Haghani, S. Samuel, and M. A. Knodler, "Real-time prediction and avoidance of secondary crashes under unexpected traffic congestion," *Accid. Anal. Prev.*, vol. 112, pp. 39-49, Mar 2018, doi: 10.1016/j.aap.2017.11.025.
- [55] Z. Pu, Z. Li, R. Ke, X. Hua, and Y. Wang, "Evaluating the Nonlinear Correlation between Vertical Curve Features and Crash Frequency on Highways Using Random Forests," *JTE, Part A: Systems*, vol. 146, no. 10, p. 04020115, 2020/10/01 2020, doi: 10.1061/JTEPBS.0000410.
- [56] L. Wang, M. Abdel-Aty, J. Lee, and Q. Shi, "Analysis of real-time crash risk for expressway ramps using traffic, geometric, trip generation, and socio-demographic predictors," *Accid. Anal. Prev.*, vol. 122, pp. 378-384, 2019/01/01/ 2019, doi: <https://doi.org/10.1016/j.aap.2017.06.003>.
- [57] R. Yu and M. Abdel-Aty, "Utilizing support vector machine in real-time crash risk evaluation," *Accid. Anal. Prev.*, vol. 51, pp. 252-259, 2013/03/01/ 2013, doi: <https://doi.org/10.1016/j.aap.2012.11.027>.
- [58] J. Yuan, M. Abdel-Aty, Y. Gong, and Q. Cai, "Real-Time Crash Risk Prediction using Long Short-Term Memory Recurrent Neural Network," *Transp. Res. Rec.*, vol. 2673, no. 4, pp. 314-326, 2019/04/01 2019, doi: 10.1177/0361198119840611.
- [59] Q. Zeng and H. Huang, "A stable and optimized neural network model for crash injury severity prediction," *Accid. Anal. Prev.*, vol. 73, pp. 351-358, 2014/12/01/ 2014, doi: <https://doi.org/10.1016/j.aap.2014.09.006>.
- [60] B. D. Greenshields, J. Bibbins, W. Channing, and H. Miller, "A study of traffic capacity," in *HRB Proc.*, 1935, vol. 14, no. 1: Washington, DC, pp. 448-477.
- [61] H. Greenberg, "An analysis of traffic flow," *Oper. Res.*, vol. 7, no. 1, pp. 79-85, 1959.
- [62] F. L. Hall, B. L. Allen, and M. A. Gunter, "Empirical analysis of freeway flow-density relationships," *Transp. Res. Part A: General*, vol. 20, no. 3, pp. 197-210, 1986.
- [63] N. Nadimi, S. S. NaserAlavi, and M. Asadamraji, "Calculating dynamic thresholds for critical time to collision as a safety measure," *Proc. Inst. Civ. Eng. - Transp.*, vol. 175, no. 7, pp. 403-412, 2022, doi: 10.1680/jtran.19.00066.



Tianheng Zhu received the B.S. degree in transportation engineering from Tongji University, Shanghai, China, in 2023.

He is currently pursuing the Ph.D. degree and working as a Graduate Research Assistant with the Lyles School of Civil Engineering, Purdue University. His current research interests include traffic safety and traffic operations and control.

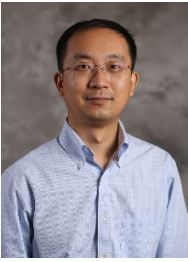
Mr. Zhu has published several papers at top conferences like IEEE ITSC and TRB Annual Meeting.



Ling Wang received the Ph.D. degree in transportation engineering from the University of Central Florida in 2016.

She is currently an Associate Professor at Tongji University, Shanghai, China. Her research interests include traffic safety, active traffic management, and big data analytics.

Prof. Wang has published more than 40 papers in top journals. She has received the Best Paper Award of World Transportation Congress and the Best Young Researcher Award of TRB as the first author.



Yiheng Feng (Member, IEEE) received the B.S. and M.E. degrees from the Department of Control Science and Engineering, Zhejiang University, Hangzhou, China, in 2005 and 2007, respectively, and the Ph.D. degree in systems and industrial engineering from the University of Arizona in 2015.

He is currently an Assistant Professor with the Lyles School of Civil Engineering, Purdue University. His research interests include traffic operations and control, cybersecurity of the transportation systems and connected and automated vehicle testing and evaluation.

Prof. Feng has published more than 50 research articles, which appeared in top journals, including Nature Communications, Transportation Research Part B/C, and IEEE Transactions on ITS. He is a member of traffic signal systems committee (ACP25) at Transportation Research Board, and co-chair of the simulation subcommittee. He is an editorial board member of Transportation Research Part C. He is the recipient of several best paper awards such as INFORMS and NDSS, and the inaugural best dissertation award from the Chinese Overseas Transportation Association (COTA).



Wanjing Ma received the Ph.D. degree in traffic engineering from Tongji University, Shanghai, China, in 2007.

He is currently a Professor and the Head of the College of Transportation Engineering, Tongji University. His research interests include traffic operation and control, intelligent transportation systems, and shared mobility.

Prof. Ma has published more than 100 articles in top journals. He was awarded the title of Elsevier Highly Cited Researcher in China in 2021.



Mohamed Abdel-Aty (Senior Member, IEEE) received the Ph.D. degree in civil engineering from the University of California, Davis, in 1995.

He is currently a Pegasus Professor and the Chair of the Civil, Environmental, and Construction Engineering Department, University of Central Florida, Orlando, FL, USA. His main expertise and interests are in the areas of ITS, simulation, CAV, and active traffic management.

Prof. Abdel-Aty has managed over 75 research projects. He has published more than 750 papers, more than 400 in journals (As of August 2023, Google Scholar citations: 29741, H-index: 95). He received nine best paper awards from ASCE, TRB, and WCTR. He is the Editor-in-Chief Emeritus of *Accid. Anal. Prev.*.